

Production of J/ψ Mesons at HERA

Beate Naroska

on behalf of the H1 and ZEUS collaborations

Institut für Experimentalphysik

Luruper Chaussee 149

D 22761 Hamburg

E-mail:naroska@mail.desy.de

Abstract. Inelastic and diffractive production of J/ψ mesons at HERA is reviewed. The data on inelastic photoproduction are described well within errors by the Colour Singlet Model in next-to-leading order. A search for colour octet processes predicted within the NRQCD/factorisation approach is conducted in many regions of phase space. No unambiguous evidence has been found to date. Diffractive elastic production of J/ψ mesons has been measured in the limit of photoproduction ($Q^2 \simeq 0$) up to the highest photon proton center of mass energies. The increase of the cross section is described by pQCD models. At larger Q^2 , $2 \leq Q^2 \leq 100 \text{ GeV}^2$, the $W_{\gamma p}$ dependence is found to be similar to that observed in photoproduction. First analyses of data at high t , $|t| \leq 20 \text{ GeV}^2$, yield a powerlike dependence on $|t|$. A LO BFKL calculation gives a good description of the data.

1. Introduction

The main interest in leptonproduction of J/ψ mesons is a clarification of the production process. In the inelastic regime, many models have been proposed, and predictions within the theoretically favoured NRQCD/factorisation approach could not yet be identified nor could they be ruled out. In the diffractive regime, models based on pQCD have proven to work in principle and more detailed studies are underway experimentally and theoretically.

This review will cover J/ψ production at HERA in inelastic and diffractive processes. Inelastic J/ψ production at HERA has been studied in the limit of photoproduction ($Q^2 \rightarrow 0$) and for $Q^2 \gtrsim 2 \text{ GeV}^2$. Data at high Q^2 were published by the H1 collaboration [1] and new theoretical calculations are discussed in L. Zwirner's contribution [2]. Here I concentrate on photoproduction.

Diffractive elastic J/ψ production is studied with large statistics in the limit of photoproduction and also at $Q^2 \gtrsim 2 \text{ GeV}^2$, where the $W_{\gamma p}$ and Q^2 dependences are analysed. Proton dissociative data at high values of t , the momentum transfer squared at the proton vertex, are also analysed.

2. Inelastic Production of J/ψ Mesons

The data from the H1[3] and ZEUS collaborations [4] on inelastic J/ψ photoproduction are based on integrated luminosities of 22 pb^{-1} and 38 pb^{-1} , respectively, collected in the years 1996/97. The kinematic regions are characterized by $Q^2 \leq 1 \text{ GeV}^2$, $50 < W_{\gamma p} < 180 \text{ GeV}$, $0.4 < z < 0.9$ for the ZEUS data and $60 < W_{\gamma p} < 180 \text{ GeV}^2$, $0.3 < z < 0.9$ for H1. The usual kinematic quantities $Q^2 = -(k - k')^2$ and $W_{\gamma p}^2 = (q + P)^2$ are used, where k , k' , q and P denote the four-momenta of the incoming and outgoing electron, of the exchanged photon and the incoming proton, respectively. An important variable is

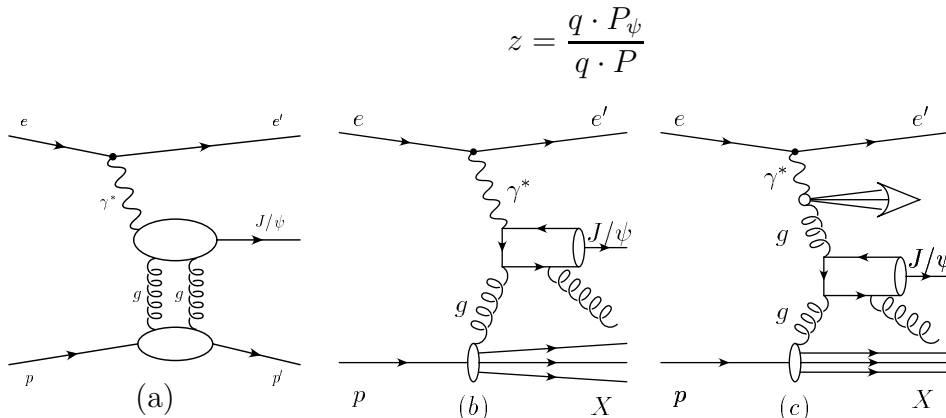


Figure 1. Generic diagrams for J/ψ production mechanisms at HERA: a) diffractive elastic process with two gluon exchange. Inelastic processes via boson gluon fusion with b) direct and c) resolved photons.

where P_ψ is the four-momentum of the J/ψ meson. In the proton rest frame z is the relative energy of the J/ψ with respect to the photon, $z \approx \frac{E_\psi^*}{E_\gamma^*}$. The variable z is used to distinguish diffractive processes, where $z \approx 1$, from inelastic processes, where $z \lesssim 0.9$.

The inelastic production process at HERA is dominated by boson gluon fusion, see Figure 1b,c. At medium z , direct processes dominate, where the photon couples directly to the charm quark, while at small z resolved photon processes are expected to contribute, where the photon interacts via its hadronic component.

The theoretical description of J/ψ meson production has undergone a change in the last few years. The Colour Singlet Model (CSM) [6] has been replaced by an effective field theory approach: non-relativistic QCD (NRQCD) and factorisation [7]. This approach contains the CSM but predicts additional contributions. In the CSM, the $c\bar{c}$ pair is produced in the hard scattering with the observed quantum numbers of the J/ψ meson. The colour singlet state is achieved by emission of an additional gluon, i.e. the process is $\gamma g \rightarrow g + c\bar{c} [1,^3S_1]^\ddagger$. In the NRQCD/factorisation approach the $c\bar{c}$ pair can also be in a colour octet state where different angular momentum states are also allowed.

At HERA we are in a unique position since for photoproduction full next-to-leading order calculations are available in the colour singlet model, which reduces the

\ddagger The ‘1’ or ‘8’ denote the colour state of the $c\bar{c}$ pair and spectroscopic notation is used for the angular momentum, $^{2S+1}L_J$.

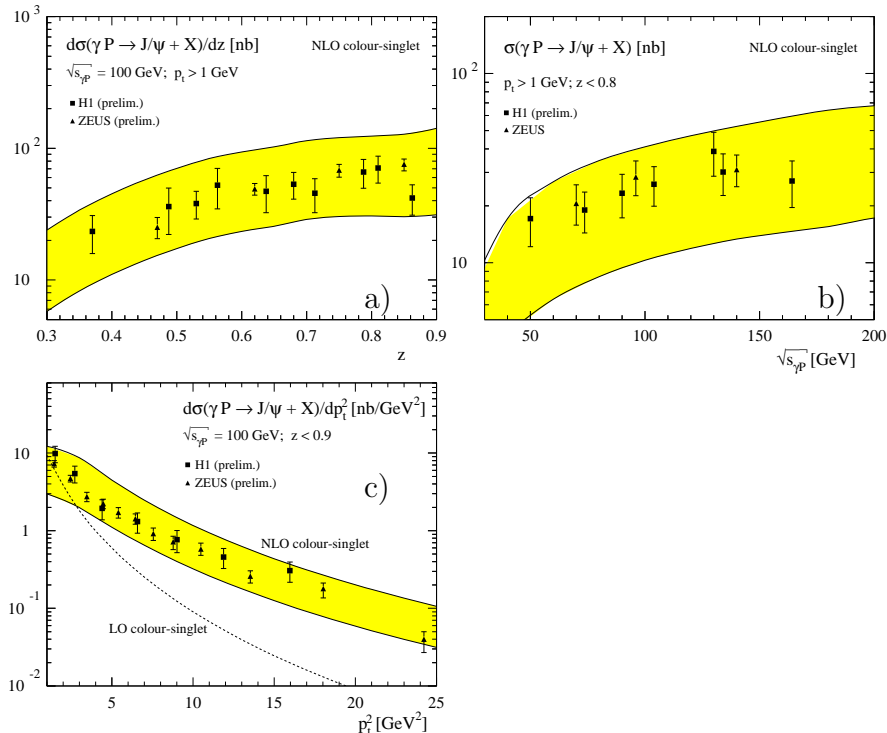


Figure 2. Cross sections as functions of z , $W_{\gamma p}$, and $p_{t,\psi}^2$. The data from H1 [3] and ZEUS [5, 4] are shown with NLO CSM calculations. The band reflects the uncertainty due to the charm mass ($1.3 < m_c < 1.5$ GeV) and $0.1175 < \alpha_s(M_Z) < 0.1225$. The renormalisation and factorisation scales are $\mu^2 = 2m_c^2$. (Figures from [8].)

uncertainties in the normalisation of the predictions. So we will first show a comparison of the data with these calculations before we address possible contributions of colour octet (CO) intermediate states.

2.1. Comparison of data to Colour Singlet calculations

In Figure 2a,b the z and the $W_{\gamma p}$ distribution are shown for data from ZEUS [4] and H1 [3] which agree well with each other. The prediction of the CSM in next-to-leading order [8] is overlaid. The band reflects the major theoretical uncertainties as detailed in the figure caption. A good description of the data is achieved. The necessity of including NLO contributions is demonstrated in the distribution of $p_{t,\psi}^2$ in Figure 2c. The theoretical band including NLO contributions describes the data well and is, at a $p_{t,\psi} \sim 4$ GeV, roughly a factor of 10 above the LO prediction. The discrepancy found in $p\bar{p} \rightarrow J/\psi + X$ at values of $p_t \sim 20 - 30$ GeV between the data and the LO CSM calculation which led to the introduction of CO contributions within the NRQCD/factorisation approach was approximately a factor ~ 40 [9].

A different approach to describe the data within the CSM is shown in Figure 3. Here the H1 data are shown with the results of two Monte Carlo implementations

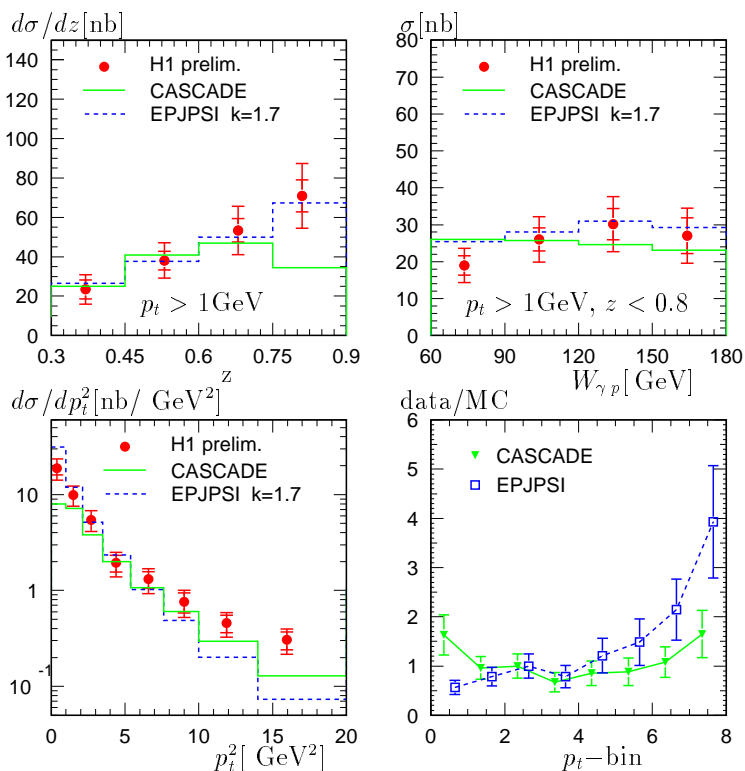


Figure 3. Differential cross sections for photoproduction of J/ψ mesons as functions of z , $W_{\gamma p}$ and p_t^2 and the ratio of Data/MC for the p_t^2 bins, normalized in the third bin. The predictions are from the CCFM Monte Carlo generator CASCADE and the Colour Singlet Model EPJPSI (the latter scaled by a factor 1.7) are compared to H1 data with $p_t > 1$ GeV and $z < 0.8$.

of the Colour Singlet Model in leading order. The dashed histograms represent the prediction from the EPJPSI [10] program which uses “standard” parton distributions integrated over the transverse momentum and evolved with DGLAP equations. The program CASCADE [11] uses the CCFM evolution equation and “unintegrated” parton distributions. These have a distribution in transverse momentum, k_t , and are obtained from a fit to H1 data on F_2 . The J/ψ data in Figure 3 (note that now a cut $z < 0.8$ has been applied) are in general well described by the CASCADE model except at very large z values, where relativistic corrections are missing. The $p_{t,\psi}^2$ distribution of CASCADE agrees better with the data than EPJPSI, but there is still a systematic discrepancy towards high p_t .

2.2. Search for Colour Octet Contributions

In Figure 4a the same differential cross sections, $d\sigma/dz$ from the H1 and ZEUS data as before, are shown again as function of z . The theoretical predictions within the NRQCD/factorisation approach in leading order [8] are shown in comparison. These include the direct photon contributions as well as resolved processes. At $z \gtrsim 0.3$, direct photon contributions dominate and the CO contribution is dominant at $z \gtrsim 0.6$. The uncertainties of the summed prediction, shown as a band, are mainly due to the uncertainties of the long range matrix elements, the parameters which, in the NRQCD/factorisation approach describe the transition of the $c\bar{c}$ state to a physical J/ψ meson.

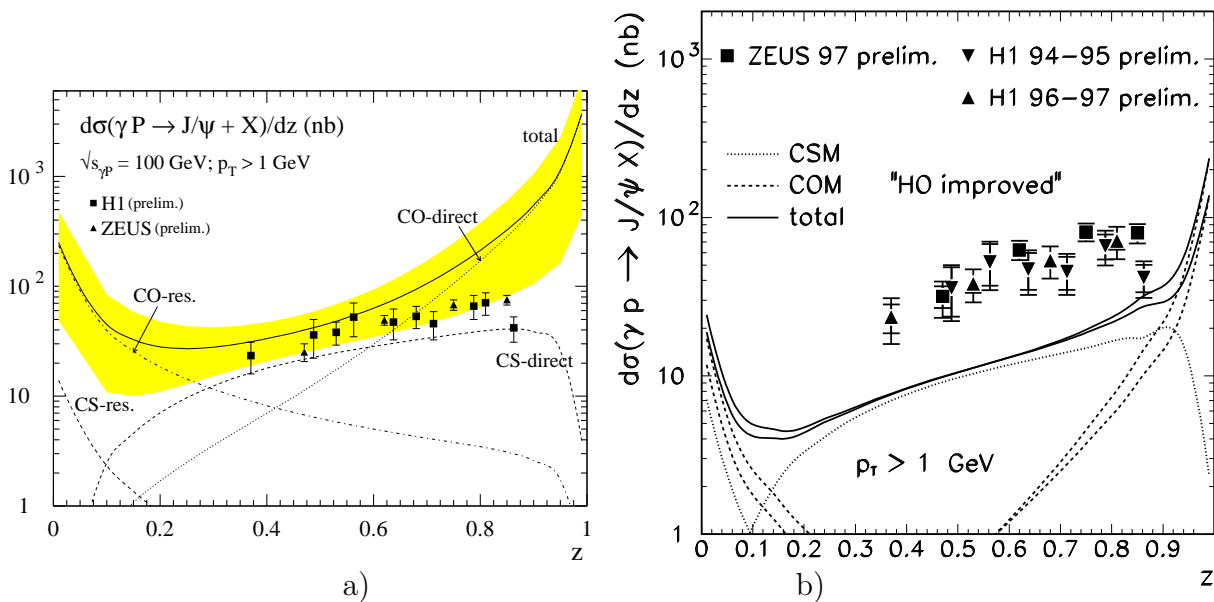


Figure 4. Differential cross section for photoproduction of J/ψ mesons as a function of z . In a) the predictions from Kraemer [8] are shown, in b) those from Kniehl et al. [12]. Both predictions include direct and resolved contributions, but use different parameters. The band in a) depicts the uncertainties which are mainly due to the long range matrix elements. In b) the uncertainties are indicated by the upper and lower curves.

$$M_k = \mathcal{O}^\psi[8,^1 S_0] + k \mathcal{O}[8,^3 P_0]/m_c^2 (10^{-2} \text{ GeV}^3)$$

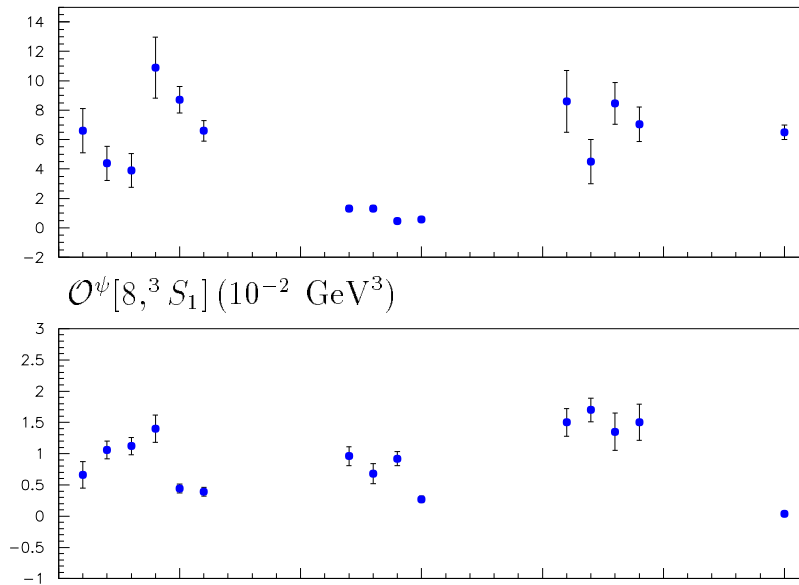


Figure 5. Long range matrix elements as compiled in [8]. The values are extracted from the transverse momentum distribution in $p\bar{p}$ J/ψ production using different theoretical approximations. Only statistical errors are shown. For more details see text.

The long range matrix elements are denoted as e.g. $\mathcal{O}^\psi[8,^3 S_1]$ to describe the transition of the $c\bar{c}$ state in a colour octet configuration with angular momentum state $^3 S_1$. They are not calculable but are believed to be universal. Numerical values have been determined in a number of theoretical analyses of $p\bar{p}$ data from the CDF collaboration using different approximations (see [8] for a summary and references). The most important matrix elements for photoproduction are $\mathcal{O}^\psi[8,^1 S_0]$ and $[8,^3 P_J]$ which are derived in the form of a linear combination $M_k = \mathcal{O}^\psi[8,^1 S_0] + k \mathcal{O}^\psi[8,^3 P_0]/m_c^2$, where k is a parameter of order 3. In Figure 5, the values for M_k (upper part) and the matrix element $\mathcal{O}^\psi[8,^3 S_1]$ (lower part) extracted by a few groups using different approximations are shown following a compilation in [8]: the first group of 6 values is calculated in the LO collinear approximation. In the second group effects of higher orders have been taken into account approximately by using a parton shower Monte Carlo model (PYTHIA). The third group uses a k_t distribution for the gluon and the last value in Figure 5 is derived in the k_t factorisation approach.

The theoretical band in Figure 4a is calculated for $(1 < M_k < 10) \cdot 10^{-2} \text{ GeV}^3$ and $(0.3 < \mathcal{O}^\psi[8,^3 S_1] < 2.0) \cdot 10^{-2} \text{ GeV}^3$ almost covering the full range of uncertainty. The strong rise predicted at large z values ($z \gtrsim 0.7$) is not seen in the data which has led to several theoretical attempts for an explanation. In Figure 4b calculations of a different group [12] are compared to the same data as in 4a. The authors of [12] attempt to estimate effects of higher orders. Here the data are a factor 3 above the predicted sum of singlet and octet contributions for $z \lesssim 0.7$, while in Figure 4a the data are below

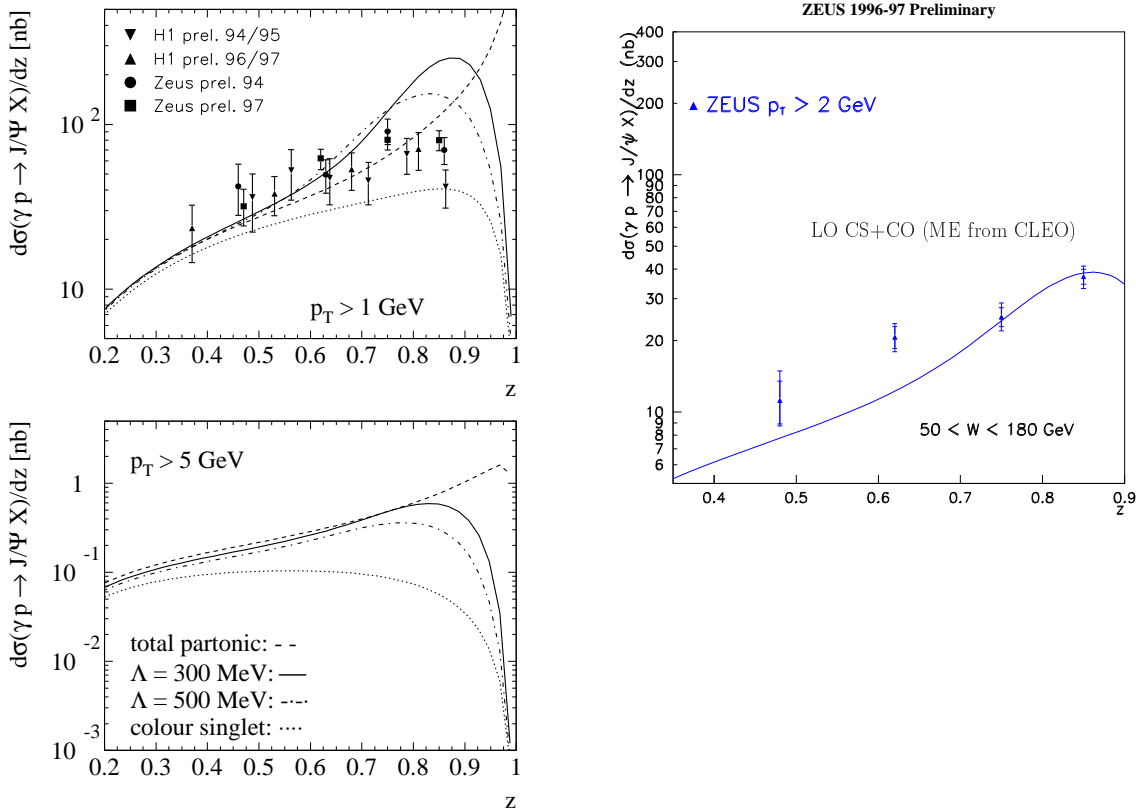


Figure 6. Left panels: Resummation of NRQCD contributions near $z \simeq 1$ according to [13]. In the upper panel predictions for $p_t > 1$ GeV are shown and compared to data. In the lower panel a cut of $p_t > 5$ GeV is applied. right panel: Comparison of the cross section $d\sigma/dz$ for $p_t > 2$ GeV from the ZEUS Collaboration with a prediction from [13] using shape functions and $\Lambda = 300$ MeV.

the final calculation. The rise in z due to CO contributions in Figure 4b takes place at $z \gtrsim 0.9$. This large z region is dominated by diffraction and no experimental results on inelastic processes are available. An intriguing question is of course a possible relation of such CO contributions with what is traditionally attributed to diffraction.

The NRQCD calculations shown in Figure 4a and b neglect the energy smearing of the transition of the $c\bar{c}$ state to the J/ψ via emission of soft gluons. This effect is expected to be large at $z \rightarrow 1$. In [13], an attempt was made to calculate this smearing using the technique of shape functions known from calculations in decays of $B \rightarrow J/\psi + X$. The calculations for the z distributions are shown together with the data in Figure 6 §. In this comparison the standard cut $p_t > 1$ GeV is applied. The smeared calculations are given for two values of Λ and show the expected decrease towards $z \rightarrow 1$ while the unsmeared curve (labelled “total partonic” in the figure) is seen to rise. However before decreasing the smeared curves are observed to increase above the unsmeared one (around $z \gtrsim 0.5$). The authors of [13] conclude that the

§ The authors also extract the long range transition matrix elements from B decays. The values, which were used for Figure 6, agree approximately with the values derived from the p_t distribution of J/ψ mesons in $p\bar{p}$ collisions taking into account higher orders via a PYTHIA Monte Carlo simulation [14].

theory is not well behaved and suggest applying a higher p_t cut. Their prediction for $p_t > 5$ GeV is shown in the lower part of the figure. A comparison of this calculation with ZEUS results for a cut $p_t > 2$ GeV is shown in the right panel of Figure 6 and is seen to give an acceptable description of the data.

2.3. Resolved Contributions and Polarisation Analysis

The region of low z values, $z < 0.45$, is explored in an analysis of H1 covering a region $130 < W_{\gamma p} < 250$ GeV and $p_t > 1$ GeV. The result is shown in Figure 7a in comparison to predictions from [12]. At such low z values, resolved photon contributions are expected and CO contributions are much larger than CS contributions. Here the smearing effects of soft gluon emission are not expected to play an important rôle. The number of parameters entering this comparison is larger and probably a mere cross section measurement will not suffice to distinguish between models. This can be judged from Figure 7b, where the predictions within the CSM are shown with the dominant uncertainties, which overall amount to a factor 5. The p_t distribution of the data is shown in Figure 7c and looks – at least with present errors – very similar to the form found at medium z values shown as a scaled curve.

Measurements of J/ψ polarisation in $p\bar{p} \rightarrow J/\psi + X$ were advocated to give independent proof of the presence of colour octet contributions. The polarisation is measured via the angular distribution of the J/ψ decay leptons in the rest frame of the J/ψ meson. Parametrising it as $1 + \alpha \cos^2 \theta$, $\alpha = +1(-1)$ corresponds to transverse (longitudinal) polarisation, while $\alpha = 0$ reflects no polarisation. The data for J/ψ and ψ' from the CDF collaboration [9], though limited in statistics, do not show the expected increase of the polarisation parameter α towards higher p_t predicted within NRQCD[17].

ZEUS performed a first measurement of the J/ψ polarisation in γp scattering. Using the flight direction of the J/ψ in the laboratory system as a reference axis the results in Figure 8a were obtained. They are compared with the predictions of the “semihard” model [18] using unintegrated gluon density distributions based on BFKL evolution equations. The trend of the data is described within this model. There are no calculations within NRQCD/factorisation which one can compare directly with the data. In Figure 8b, calculated in the “recoil” system which uses the J/ψ direction in the γp system as a reference axis, one can however see that the α parameter increases with $p_{t,\psi}$ for the Colour Singlet Model while it remains small for the octet contributions.

Summarising, there is still no evidence of colour octet contributions in photoproduction at HERA. Due to the experimental and theoretical uncertainties they can however not be excluded.

3. Diffractive Production of J/ψ Mesons

In the last few years it has been demonstrated that elastic J/ψ production can be described by perturbative QCD in photoproduction and also at finite Q^2 . Data for

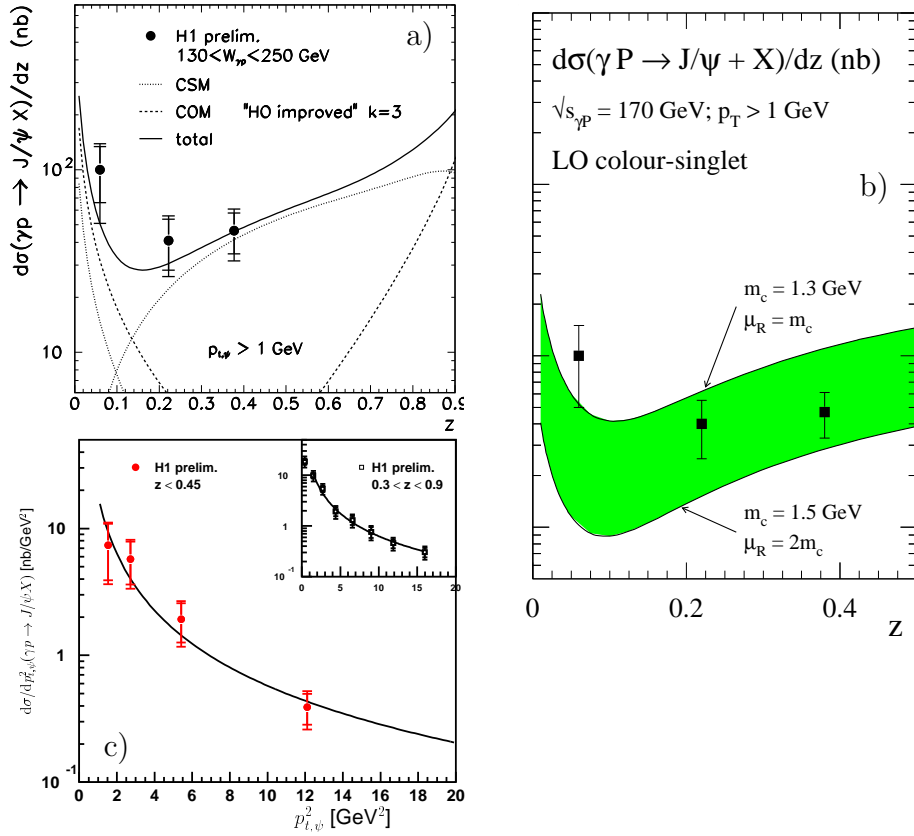


Figure 7. Photoproduction of J/ψ mesons at low z from H1. Note the changed $W_{\gamma p}$ range compared to medium z . The theoretical predictions for the z distribution in a) are from Kniehl *et al* [12]. In b) the same H1 data are shown with a LO calculation within the CSM from [8] depicting the major uncertainties. c) $d\sigma/dp_t^2$ in the low z regime. The curve is a scaled fit to the medium z data.

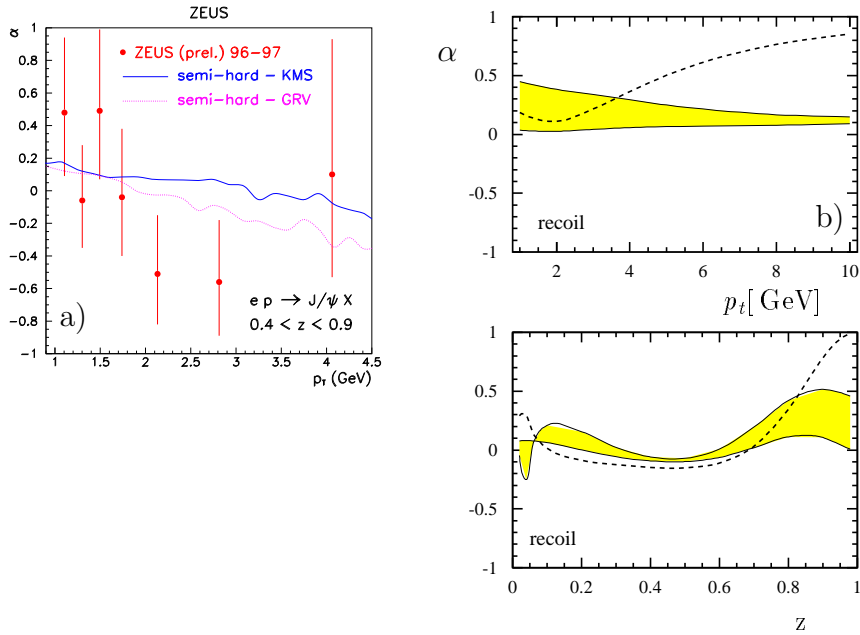


Figure 8. a) The polarisation parameter α as a function of the transverse momentum of the J/ψ meson measured by the ZEUS collaboration [15]. b) Theoretical predictions for α within the CSM (dashed curve) and the Colour Octet Model as functions of p_t [15]. Note that the dashed curve is the LO prediction and the solid curve is the NLO prediction.

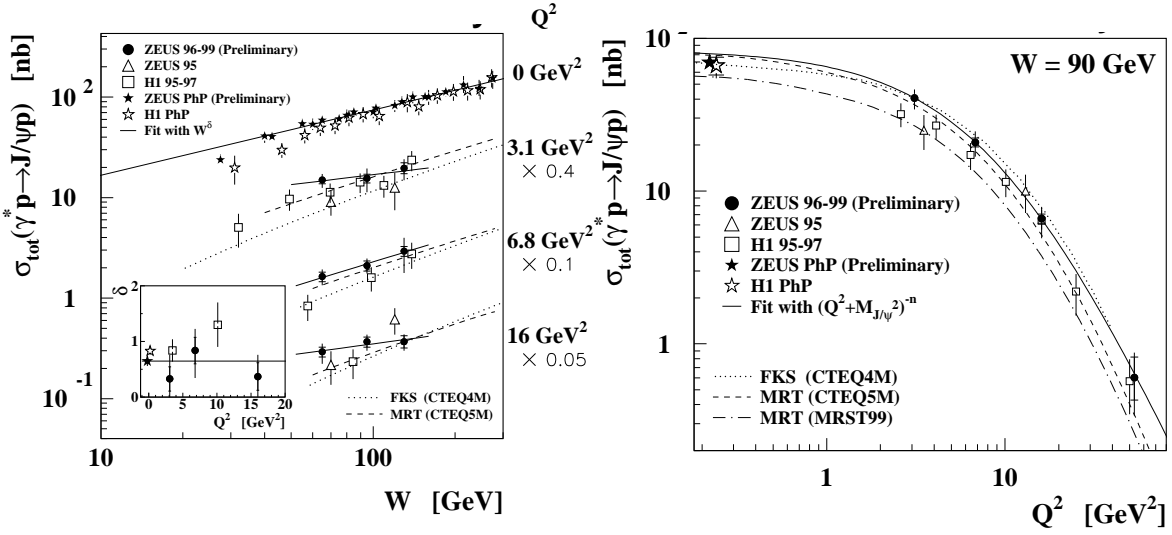


Figure 9. Elastic photoproduction of J/ψ mesons as a function of $W_{\gamma p}$ (left) and Q^2 (right). The data from H1 and ZEUS are shown with fits to the data as well as predictions within two pQCD models.

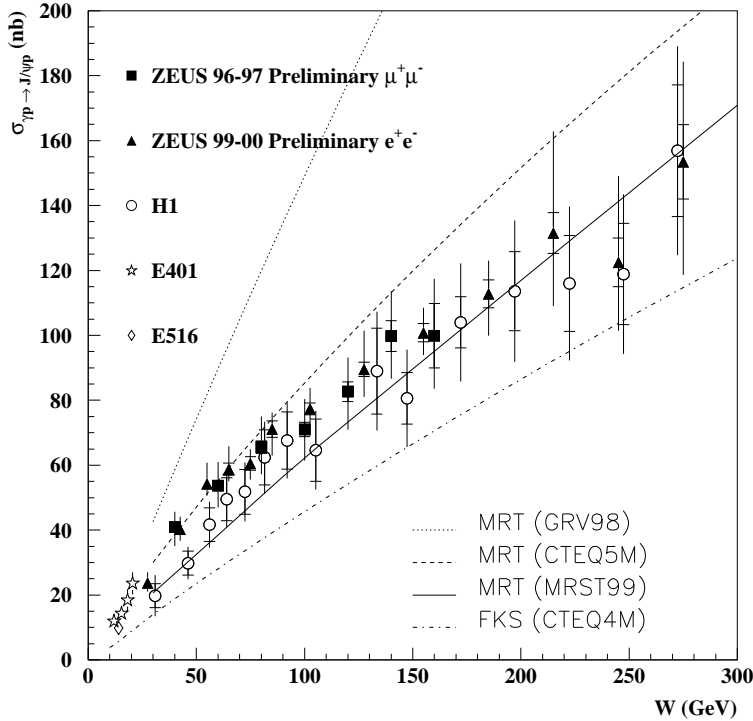


Figure 10. Elastic photoproduction of J/ψ mesons: the data from H1 and ZEUS are shown with two different theoretical predictions within pQCD using different parton distributions.

elastic diffractive processes are now available in a large kinematic range. A summary of the published H1 data (21 pb^{-1}) [1, 19] and the new preliminary data from ZEUS [20] (corresponding to $\sim 40 \text{ pb}^{-1}$) are shown in Figure 9. The data cover the regime of photoproduction, $Q^2 \rightarrow 0$, extending almost to the kinematic limit in the photon proton energy $W_{\gamma p} \leq 300 \text{ GeV}$. In Q^2 the data go up to $\sim 100 \text{ GeV}^2$.

The curves in Figure 9 show fits to the data of the form W^δ and δ is also plotted as a function of Q^2 in the insert of Figure 9. The value of δ is on average well above ~ 0.22 expected from Regge-type fits with a soft pomeron. The Q^2 distribution is fitted by a functional form $(Q^2 + M_\psi^2)^{-n}$, yielding $n = 2.38 \pm 0.11$ for H1 and $n = 2.60 \pm 0.11_{-0.05}^{+0.08}$ for the ZEUS data.

The photoproduction data in Figure 10 are overlaid with predictions from two theoretical groups using different approaches within pQCD [21, 22]. The basic picture is the exchange of two gluons between the proton and the $c\bar{c}$ pair. Apart from a number of technical differences the groups handle the conversion to a J/ψ meson differently: MRT use parton-hadron duality, while FKS use a wave function.

The important prediction is for the slope of the data which is described well by all calculations shown with the exception of GRV98 partons. H1 has previously also found good agreement within the FKS calculations using CTEQ4M or MRSR2 partons [19].

Both collaborations have extracted the effective trajectory from photoproduction data. The procedure is to fit the data at fixed values of t with a form $W^{\alpha(t)-1}$. The resulting values of $\alpha(t)$ are displayed in Figure 11 with separate fits to a simple form $\alpha(0) + \alpha't$. The more accurate ZEUS data yield $\alpha(t) = (1.193 \pm 0.011_{-0.010}^{+0.015}) + (0.105 \pm 0.024_{-0.020}^{+0.022}) \cdot t$. The H1 data are compatible with this result. The soft pomeron trajectory is ruled out. A NLO BFKL calculation of the intercept $\alpha(0)$ [23] is in agreement with the data.

The data shown so far are dominated by low values of $|t|$ since they are found to drop with an exponential behaviour: $e^{-b|t|}$ with $b \approx 4 \text{ GeV}^{-2}$. Data collected at high $|t|$ are shown in Figure 12. At high values of $|t|$, the proton dissociates into a low mass system X . ZEUS and H1, at present, measure slightly different cross sections: the ZEUS data are corrected to a range $0.01 < t/(t - M_X^2) < 1$ while H1 corrects to the full kinematically allowed region of M_X . A LO calculation implementing the BFKL evolution equation [24] reproduces the data sets well using a value for $\bar{\alpha}_s \approx 0.2$.

4. Summary and Outlook

Inelastic photoproduction of J/ψ mesons at HERA continues to be well described by the Colour Singlet Model calculated in next-to-leading order. At a $p_{t,\psi} \simeq 4 \text{ GeV}$, the measured cross section is reproduced by the NLO calculation, which is a factor of 10 above the LO prediction. A reasonable alternative description of the data on a Monte Carlo basis can be obtained using parton distributions not integrated over the transverse momentum based on the CCFM evolution equations. As regards Colour Octet contributions, only LO calculations are available. Due to normalisation uncertainties,

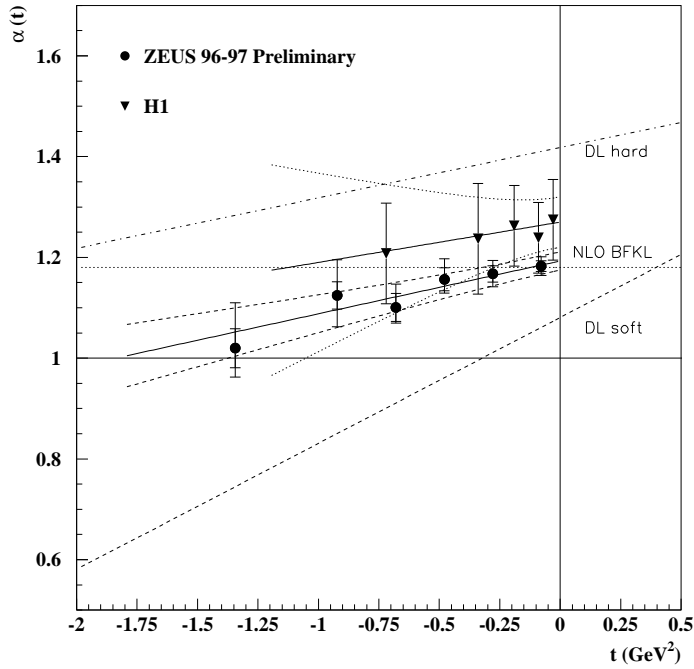


Figure 11. The effective trajectory for photoproduction of J/ψ mesons extracted from photoproduction data.

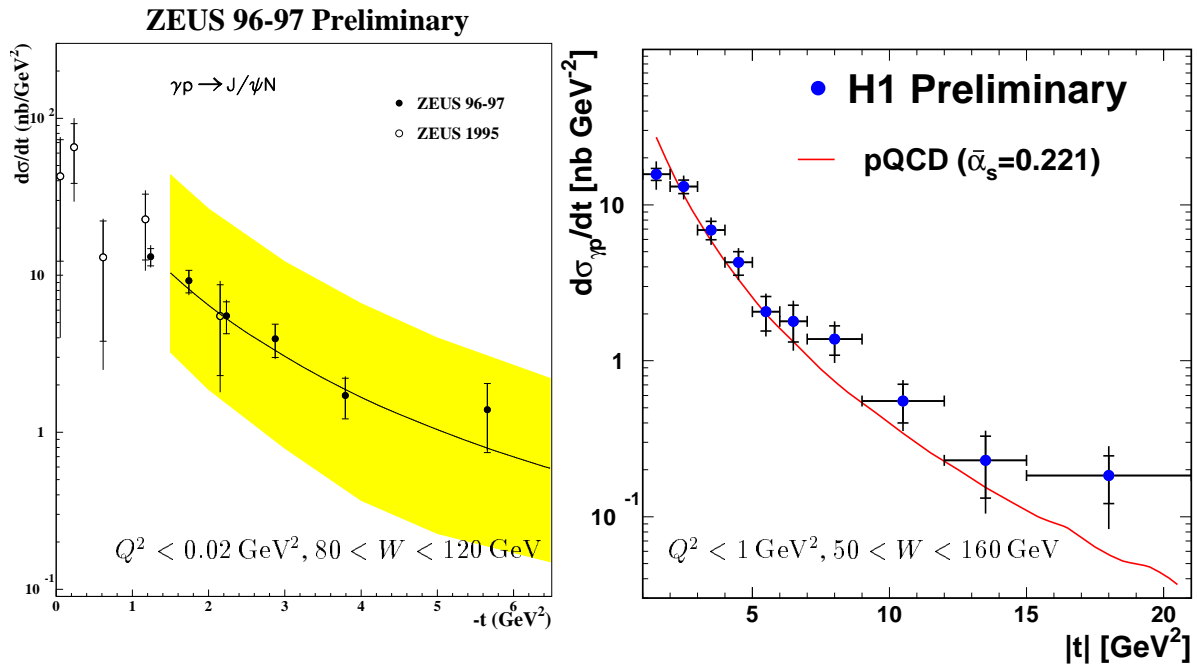


Figure 12. J/ψ Production at high values of $|t|$ in comparison with predictions from [24] using BFKL dynamics. The band around the curve on the left depicts the major uncertainties.

the comparison with data at high z values is still ambiguous. NRQCD resummations at high z seem to necessitate a higher $p_{t,\psi}$ cut and then describe the data reasonably well. A first analysis of data at low z values shows sensitivity to resolved contributions. However since in this regime more parameters enter, a mere cross section measurement may not be sufficient to decide on Colour Octet contributions. A first attempt to measure the J/ψ meson polarisation looks promising. This and all other analyses will profit from the increased statistics which will soon become available.

For elastic J/ψ production, the $W_{\gamma p}$ range in photoproduction has been extended almost to the kinematic limit. The cross section continues to rise. Parametrising it as $W_{\gamma p}^\delta$, δ is measured to be large, of order 0.8. The data at higher Q^2 are in rough agreement with such a steep rise. Comparisons of theoretical calculations within pQCD show a sensitivity to the gluon distribution. A “trajectory” measurement excludes the soft pomeron trajectory. The measurement of diffractive processes has been extended to $|t|$ values of ~ 20 GeV². The data is well described by calculations based on the BFKL equation.

Acknowledgement I wish to thank the organizers for letting me participate in this very fruitful and stimulating meeting in beautiful surroundings. Thanks to all ‘theoretical’ and ‘experimental’ colleagues for discussions about their data or theories!

- [1] H1 Coll., C. Adloff *et al.*, *Eur. Phys. J. C* **10** (1999) 373 [hep-ex/9903008].
- [2] L. Zwirner, these proceedings.
- [3] H1 Coll., “Inelastic Photoproduction of J/ψ and ψ' at H1”, contributed paper to International Europhysics Conference on High Energy Physics HEP99, 1999, Tampere, Finland; “Inelastic Photoproduction of J/ψ Mesons at Low z ”, contributed paper to ICHEP2000, International Conference on High Energy Physics 2000, Osaka, Japan
- [4] ZEUS Coll., “Measurement of Inelastic J/ψ Photoproduction at HERA”, Contributed paper 814 to International Conference on High Energy Physics, ICHEP98, Vancouver, July 1998; “Inelastic J/ψ Photoproduction at HERA”, contributed paper to ICHEP2000, International Conference on High Energy Physics 2000, Osaka, Japan
- [5] ZEUS Coll., J. Breitweg *et al.* *Z. Phys.* C76 599 (1997)
- [6] Berger E.L. and Jones D., *Phys. Rev.* D23, 1521 (1981); Baier R. and Rückl R., *Phys. Lett.* B102, 364 (1981); *Nucl. Phys.* B201, 1 (1982); *Z. Phys.* C19, 251 (1983)
- [7] G.T. Bodwin, E. Braaten, G.P. Lepage, *Phys. Rev. D* **51**, 1125 (1995), erratum *Phys. Rev. D* **55**, 5853 (1997).
- [8] Krämer M., hep-ph/0106120, to be published in Progress in Particle and Nuclear Physics, Vol. 47, issue 1; *Phys. Lett.* B348, 657 (1995); *Nucl. Phys.* B459, 3 (1996)
- [9] CDF Coll., Abe F. *et al.*, *Phys. Rev. Lett.*, 69, 3704 (1992); *ibid.* 79, 572 (1997); DØ Coll., Abachi S. *et al.*, *Phys. Lett.* B370, 239 (1996)
- [10] Jung H., Krücker D., Greub C. and Wyler C., *Z. Phys.* C60, 721 (1993)
- [11] H. Jung and G.P. Salam, *Eur. Phys. J. C* **19** (2001) 351
- [12] Kniehl B.A. and Kramer G., *Phys. Rev.* D56, 5820 (1997); *Phys. Lett.* B413, 416 (1997); *Eur. Phys. J. C* **6**, 1999 (493)
- [13] M. Beneke, G. A. Schuler and S. Wolf, *Phys. Rev. D* **62** (2000) 034004 [hep-ph/0001062].
- [14] Cano-Coloma B. and Sanchis-Lozano M.A., *Nucl. Phys.* B508, 753 (1997)
- [15] ZEUS Coll., talk by R. Brugnera at DIS2001, Bologna

- [16] Beneke M. and Krämer M., *Phys. Rev. D* **55**, 5269 (1997);
Beneke M., Rothstein I.Z. and Wise M.B., *Phys. Lett. B* **408**, 373 (1997)
- [17] CDF Coll., T. Affolder *et al.*, *Phys. Rev. Lett.* **85** (2000) 2886 [hep-ex/0004027].
- [18] S. P. Baranov, *Phys. Lett. B* **428** (1998) 377.
- [19] H1 Coll., C. Adloff *et al.*, *Phys. Lett. B* **483** (2000) 23 [hep-ex/0003020].
- [20] ZEUS Coll., “Exclusive Photoproduction of J/ψ Mesons”, contributed paper 878 to ICHEP2000, International Conference on High Energy Physics 2000, Osaka , Japan; “Exclusive Electroproduction of charmonium at HERA”, *ibid.* paper 879
- [21] L. Frankfurt, W. Koepf and M. Strikman, *Phys. Rev. D* **57** (1998) 512 [hep-ph/9702216].
- [22] A. D. Martin, M. G. Ryskin and T. Teubner, *Phys. Lett. B* **454** (1999) 339 [hep-ph/9901420];
Phys. Rev. D **62** (2000) 014022 [hep-ph/9912551].
- [23] S.J. Brodsky *et al.*, *JETP Lett.* **70** (1999) 155
- [24] J. Bartels, J. R. Forshaw, H. Lotter, L. N. Lipatov, M. G. Ryskin and M. Wusthoff, *Phys. Lett. B* **348** (1995) 589 [hep-ph/9501204]; J. R. Forshaw and M. G. Ryskin, *Z. Phys. C* **68** (1995) 137 [hep-ph/9501376].